

Microscale mechanisms of ultrasound velocity measurement in metal melts

Bitong Wang, Douglas H. Kelley*

University of Rochester, Rochester, NY, 14627, USA

ARTICLE INFO

Keywords:

Ultrasound velocity measurement
Ultrasound doppler velocimetry
Liquid metals
Gallium
Echo deterioration
Indirect-contact measurement

ABSTRACT

Ultrasound Doppler velocimetry (UDV) is a powerful, widely used technique for measuring flow in metal melts. However, UDV in metal melts suffers from substandard reliability because its operation depends on phenomena that are poorly understood. In this study, we investigate the poorly characterized source of bulk echoes in metal melts and the corresponding mechanisms of ultrasound signal deterioration. We present evidence from electron microscopy and ultrasound measurements that oxide inclusions are the main source of bulk echoes in gallium. By measuring their terminal velocity, we estimate the mean size of echoing objects in gallium to be 58–64 μm , implying that Mie scattering is the dominant scattering mechanism. By comparing UDV measurements in which signals were transmitted directly into the fluid, to others in which signals were transmitted through a vessel wall, we show evidence that there are two distinct mechanisms for signal degradation: the loss of echoing objects from the bulk and the deterioration of acoustic coupling and wetting at the transducer surface. We suggest stirring vigorously and using indirect-contact UDV measurement strategy to mitigate the signal degradation in metal melts.

1. Introduction

Unlike transparent liquids such as water, metal melts are incompatible with optical techniques for measuring flow. Ultrasound Doppler Velocimetry (UDV) can enable the flow measurement of opaque liquids in a non-invasive way [1–3]. In the last few decades, UDV has developed as a powerful tool and been successfully applied to many different kinds of metal melts [4–12]. The technique is widely used in various studies related to the fluid dynamics of metal melts, such as electromagnetic flow [13–22], alloy casting [23–27], solidification [28–32], liquid metal batteries [33–35], and lab-scale models for geophysical research [36–42].

The working principle of UDV is based on the pulse-echo method: ultrasound pulses are emitted by a transducer, and echoes are recorded by the same transducer or by another. Echoes are formed when ultrasound waves are reflected at large interfaces or scattered by small particles or bubbles suspended in the fluid. The position of the echoing object can be determined from the time of flight of the echo; the velocity of the echoing object can be determined from shifts in positions between consecutive pulses, or from the Doppler shift of the echo frequency. If the object is a tracer particle that accurately follows fluid motion, its velocity gives a measure of the fluid velocity at that location. If many tracer particles are present, a single pulse can produce many echoes and

therefore many measurements, yielding a velocity profile along a line in the wave propagation direction.

Obtaining high-quality ultrasound signals can be a challenge in metal melts. In UDV, velocity measurements are made from information contained in the echoes [2,3]. Thus, the quality of echo signals determines the performance and accuracy of UDV. To get sufficient echoes for velocity measurement, inhomogeneities like small particles or bubbles are required in the bulk of the fluid. For water-based fluid, bulk echoes are usually created by adding artificial tracer particles whose density nearly matches the fluid. For liquid metals or metal melts, artificial tracer particles can also be added to generate bulk echoes [5, 12,43]. However, the high surface tension of metal melts usually hinders homogeneous mixing of tracer particles in the melt [3].

Interestingly, strong bulk echoes can often be detected in metal melts even without adding tracer particles. Naturally occurring metal oxide inclusions are often assumed to be the source [6,7,19,29,30,33,42, 44–46]. However, no direct evidence concerning the relationship between metal oxides and bulk-echo signals has been provided. In fact, other common inhomogeneities like metal impurities, microbubbles, or microscopic segregations [7,17,47] might cause echoes as well. To our knowledge, no prior publication systematically investigated the source of bulk echoes in metal melts, and the mechanisms by which those inhomogeneities scatter ultrasound waves have not been explained.

* Corresponding author. 218 Hopeman Engineering Building, P.O. Box 270132, Rochester, NY, 14627-0132, USA.

E-mail addresses: bwang34@ur.rochester.edu (B. Wang), d.h.kelley@rochester.edu (D.H. Kelley).

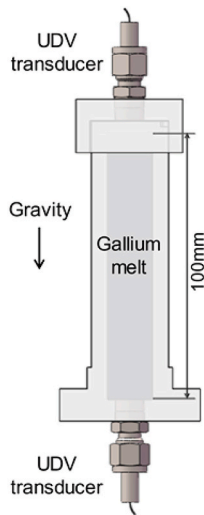


Fig. 1. Apparatus for echo source experiments: gallium melt was placed in a vertical container. UDV transducers were placed at the top and bottom.

Understanding those mechanisms would help explain the common observation that ultrasound signals in metal melts deteriorate over time [5,7,19,33]. Although some studies gave empirical advice for prolonging the ultrasound measurement time [5,19,30,33], the deterioration typically cannot be avoided even after meticulous preparation of careful experiments. The interface between the ultrasound transducer and metal melt may be the source of the trouble according to circumstantial evidence [5–7]. However, this deterioration phenomenon has not been studied in detail, and the mechanisms causing it are not yet well understood.

Gallium and its eutectic alloys are the most common materials used in ultrasound studies of metal melts due to their low melting temperatures and operational safety. In this paper, we selected gallium as the fluid to investigate the microscale mechanisms of ultrasound velocity measurement in metal melts. We combined scanning electron microscope (SEM) examinations, ultrasound measurements, and optical methods to determine the source of bulk echoes in gallium. We developed an estimation method to calculate the mean size of echoing objects in gallium melt. We applied both direct-contact and indirect-contact measurement to study the deterioration of ultrasound signals at the interface and in the bulk. In the next section, the paper continues with our experimental methods. Then, the paper presents and discusses our experiment results in detail. Finally, the paper concludes with a summary and suggestions for future work.

2. Experimental methods

To investigate the mechanisms of ultrasound measurement in gallium melt, we conducted experiments in two parts, one focused on finding the sources of bulk echoes in gallium melt, and another focused on investigating the deterioration of ultrasound signals over time in gallium.

2.1. Echo source experiments

Any impurities in a gallium melt might produce bulk echoes. To determine what impurities were present in our gallium samples, we cast a gallium sample and characterized its top surface, bottom surface, and cross section under SEM and energy-dispersive x-ray spectroscopy (EDS).

Fig. 1 shows the experimental apparatus for investigating the source of bulk-echoes in gallium melt. A vertical container made of acrylic was filled with gallium melt (from solid gallium, 99.99% purity). Two 8-MHz

ultrasound transducers (Signal Processing, Switzerland) were placed at the top of the lid and the bottom of the container. Both transducers were connected to the DOP3010 Velocimeter (Signal Processing, Switzerland) and operated in emit/receive mode for data acquisition, with operation parameters of 2 pulse length, 10000- μ s pulse repetition period, and 150 emissions per profile. DOP3010 Velocimeter was operated in energy-profile mode in which a high-pass filter is applied, so that only the echoes caused by objects moving along the ultrasound wave propagation direction were measured and recorded.

In this experiment, no artificial flow was induced, and gravity was the dominant force causing particles to move. UDV measures the movement of echoing objects along the ultrasound propagation direction inside a fluid. Therefore, the UDV transducers placed at top and bottom detected and recorded the objects' movements caused by gravity.

For comparison, similar experiments were also conducted in water containing tracer particles with known size and density. In order to verify the accuracy of UDV measurements, Particle Tracking velocimetry (PTV) was also performed in water. The UDV-PTV apparatus is shown in Supplementary Fig. S1.

2.2. Estimating the size of echoing objects

Due to the opacity of gallium, the shape and size of impurities causing echoes could not be measured directly. We developed a method to estimate the mean size of echoing objects based on the principle of terminal velocity. An object falling in a fluid reaches its terminal velocity when all forces acting on it are balanced. In our case, the forces include viscous drag, buoyancy, gravity, and the acoustic force exerted by the ultrasound transducer. The acoustic force can push echoing objects away along the wave propagation direction, but its magnitude is not known a priori. To compensate, we performed two tests using the apparatus shown in Fig. 1, with the same ultrasound transducer at top and bottom, respectively, and with the same acoustic power applied. When the transducer is placed at top, the acoustic force is in the same direction as gravity; when the transducer is placed at the bottom, the acoustic force opposes gravity. In both cases, all forces on the object must balance once it reaches terminal velocity:

$$F_{acoustic} + \frac{4}{3}\pi r^3 g(\rho_{particle} - \rho_{liquid}) = 6\pi\mu r v_{top} \quad (1)$$

$$F_{acoustic} - \frac{4}{3}\pi r^3 g(\rho_{particle} - \rho_{liquid}) = 6\pi\mu r v_{bot} \quad (2)$$

Here $F_{acoustic}$ is the acoustic force, ρ is density, g is the gravitational acceleration, r is radius of the echoing object, μ is the dynamic viscosity of the fluid, and v_{top} and v_{bot} are the measured velocity when placing the transducer at top and bottom, respectively. Both are defined as positive when particles move away from the transducer, so for a rising particle, $v_{top} < 0$ and $v_{bot} > 0$. Knowing the densities, measuring the velocities, and eliminating $F_{acoustic}$ algebraically, we can calculate r .

We made few assumptions for this estimation. First, we assumed the echoing objects were spherical, though their real shape could be irregular. Second, we assumed the echoing objects were in an equilibrium state during our measurements. Third, since UDV measures the velocity of an ensemble of echoing objects inside a measuring volume, we assumed the objects inside one measuring volume were moving with the same velocity. Fourth, we presumed that spatial attenuation of the acoustic force was negligible, which required choosing a small measurement region (see below). Fifth, we presumed that near-field effects were negligible, which required choosing a measurement region far from the transducer (see below).

To check the accuracy of this estimation method, we first tested it in water. The size of the seeded tracer particles was specified by the manufacturer and was compared to our experimental results. As an additional check, the shape and diameter of the tracer particles were

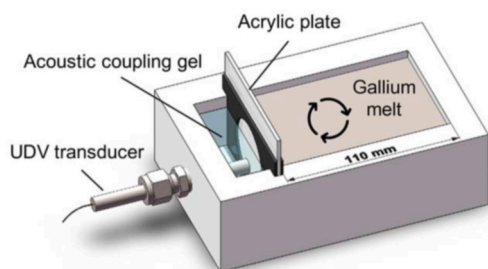


Fig. 2. Apparatus for signal deterioration experiments: ultrasound measurements were conducted through an acrylic plate, with acoustic coupling gel. Arrows mark the flow generated by a rotating magnetic field beneath the vessel. The apparatus also allowed direct-contact measurements without the plate or gel in place.

also measured under an optical microscope.

2.3. Signal deterioration experiments

Fig. 2 shows the vessel designed for investigating ultrasound signal deterioration over time in metal melt. A rotating flow was induced in the gallium melt by rotating a magnet beneath the vessel (using a laboratory stir plate, without a stir bar in the gallium). Presumably, the changing magnetic field induced eddy currents in the conductive gallium, and those currents coupled with the field to cause forces on the gallium, driving flow. For this study, the detailed structure of the flow was not important, as long as flow was measurable and repeatable. To ensure repeatability, both the position of the vessel and the rotation speed were kept constant in all tests. The ability of UDV to measure this flow accurately was used as an indicator of signal quality.

A 4 MHz UDV transducer was used in this experiment, and all measurements were carried out using the same ultrasound parameter settings. The measured bulk echo intensities, flow velocities, and back-wall echo intensities were compared among different tests.

To explore the role of the transducer/gallium interface, UDV measurements were performed either with the transducer in direct contact with the melt, or through an acrylic plate, with acoustic coupling gel between the plate and the transducer, which touched it gently. To maximize the transmission of acoustic energy, the thickness of the acrylic plate was selected to be a half-integer multiple of the ultrasound wavelength in acrylic [48]. In all tests, the transducer, vessel, acoustic coupling gel, and gallium melt were preheated to 60 °C in order to improve the stability of ultrasound signals [19].

3. Results and discussion

3.1. The source of bulk echoes in gallium

SEM images can provide information about impurities (echoing

objects) in gallium. **Fig. 3** shows gallium oxide inclusions found at the cross section and top surface of a cast gallium sample. Other than gallium oxide, we also found various of metal impurities from the sample, such as lead, bismuth, indium, and gold (**Supplementary Fig. S2**). These impurities might have been introduced into gallium during our experimental procedures or during manufacture. However they were introduced, those impurities could scatter ultrasound waves. If gravity is the only force driving the motion of echoing objects, then impurities with density less than gallium will rise, whereas impurities with density less than gallium will sink. Thus, studying the gravity-driven motion of echoing bodies in gallium can give further insight into their composition.

As shown in **Fig. 1**, two ultrasound transducers were used to measure the gravity-driven velocities of echoing objects in gallium. The measured mean velocities are plotted in **Fig. 4(a)** as a function of distance from the transducer. Here, a positive velocity means the objects are moving away from the transducer, and a negative velocity means the objects are moving toward the transducer. Thus, the negative velocity measured by the top transducer indicates objects rising, and the positive velocity measured by the bottom transducer also indicates objects rising. Measurements from both transducers agree closely, as shown in **Fig. 4 (b)**, when plotted as a function of the vessel's height, with upward velocity defined as positive.

Besides the velocity profile, we can also observe the movement of echoing objects directly from UDV energy maps. **Fig. 5** shows energy profiles, in which bright pixels indicate the positions of objects detected at different times. Trajectories appear as streaks whose slopes indicate velocities of the echoing objects. A test in water with tracer particles was conducted first, and UDV energy maps measured by the top and bottom transducers are shown in **Fig. 5(a)** and **(b)**, respectively. The trajectories of tracer particles in water clearly show that they sink, consistent with the fact that they have higher density (1.022 g/cm³) than water. In gallium, the trajectories shown in **Fig. 5(c)** and **(d)** indicate that most echoing objects rise, in agreement with the velocity measurements shown in **Fig. 4**.

Velocity profiles and UDV energy maps indicate that the echoing objects are less dense than gallium. Among the impurities we found in SEM images, only gallium oxide ($\beta\text{-Ga}_2\text{O}_3$) [49] is less dense than molten gallium (5.88 g/cm³ vs. 6.095 g/cm³). Therefore, the gallium oxide is likely the main source of bulk echoes in gallium melt.

To verify that echoing objects are primarily composed of gallium oxide, we treated gallium melt with HCl in order to reduce oxide inclusions inside gallium. Specifically, we applied HCl (1 M) on top of the gallium and manually stirred to ensure that the HCl fully reacted with any gallium oxide. Then the HCl was removed, and the cleaned gallium was left at 60 °C to dry for 1 h before UDV measurement. **Fig. 6(a)** shows pictures of the gallium surface before and after HCl treatment. For the original gallium melt, some oxide inclusions are apparent on the surface. After HCl treatment, the gallium shows a mirror-like surface, free of inclusions. **Fig. 6(b)** compares mean bulk echo intensities measured in

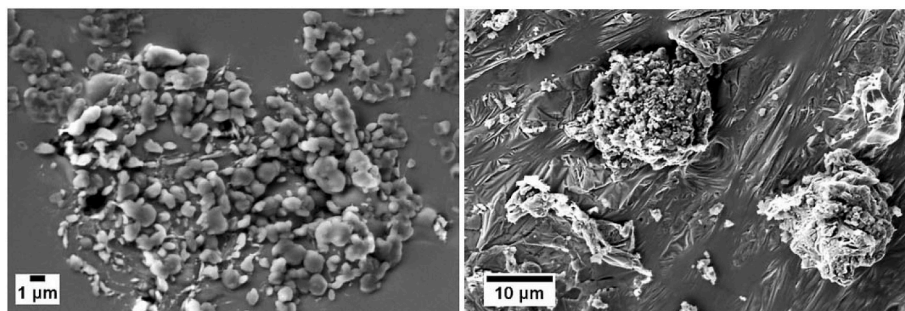


Fig. 3. SEM images of gallium oxide inclusions found at the cross section (left) and top surface (right) of a solidified gallium sample. The size of gallium oxide inclusions ranges from few microns to tens of microns.

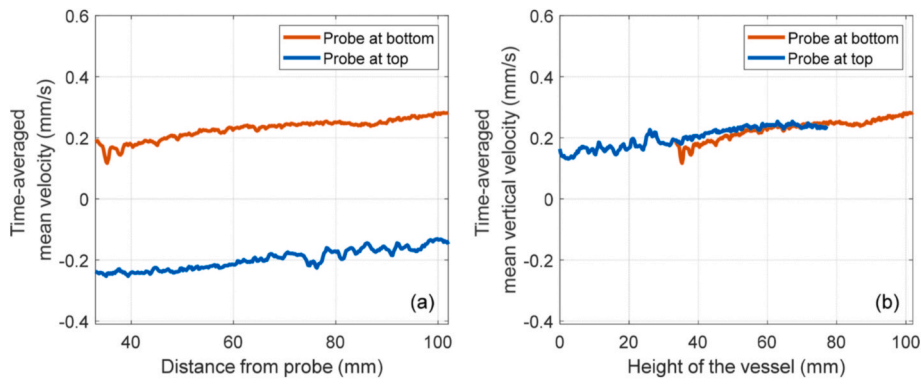


Fig. 4. UDV velocity profile measured in gallium melt. Echoing objects were allowed to sink or rise under the influence of gravity. (a) Distance from probe vs. velocity. (b) Height of vessel vs. vertical velocity. The velocity curves were obtained by averaging over 2 min of UDV measurement. Velocity measurements close to each transducer were distorted by ringing and near-field effects, and have therefore been excluded. Both plots show echoing objects rise.

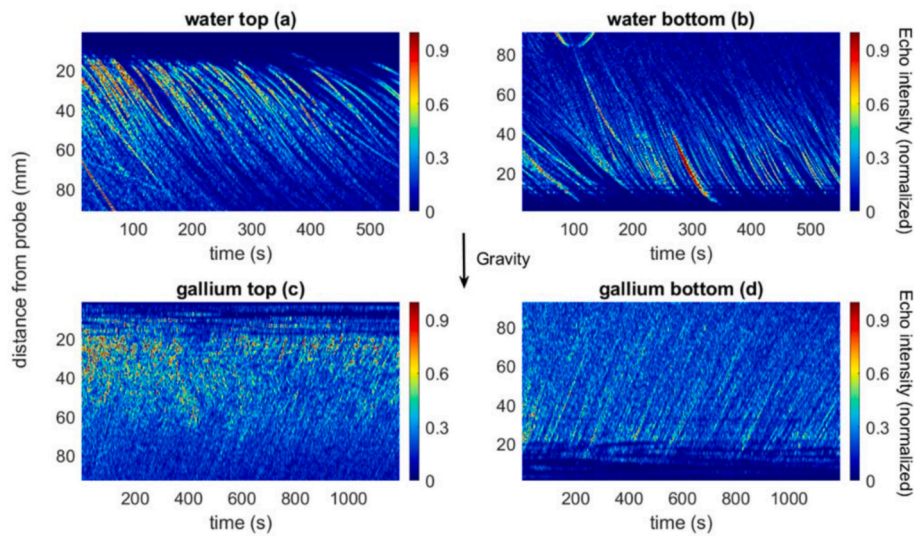


Fig. 5. UDV energy maps. Only the echoes caused by moving objects within the ultrasound beam path were measured and displayed in the maps. High-intensity streaks indicate trajectories of echoing objects. The slopes of the trajectories indicate that echoing objects move downwards in water and upwards in gallium. Echo measurements close to each transducer were distorted by ringing and near-field effects.

the original gallium and the HCl-treated gallium. After HCl treatment, the bulk echo intensity became much weaker, giving further evidence that gallium oxide is the main source of bulk echoes in gallium.

3.2. Estimating the size of echoing objects

Depending on their size, echoing objects can scatter ultrasound waves by different mechanisms. According to the size ratio of typical UDV ultrasound wavelength and echoing objects size, there are two possible scattering mechanisms: Rayleigh scattering and Mie scattering

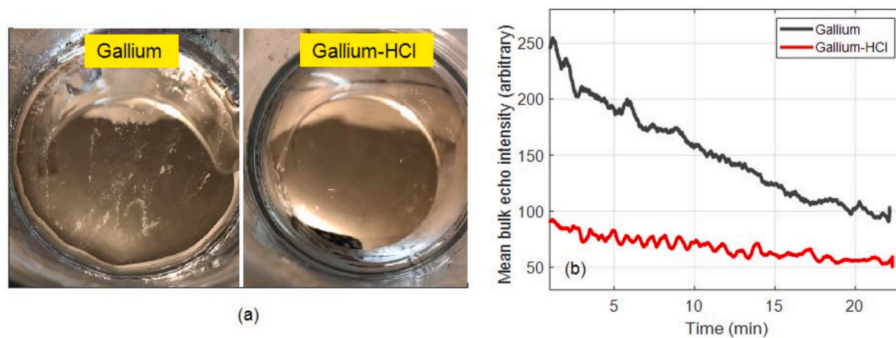


Fig. 6. HCl treatment. (a) Pictures of original gallium and HCl-treated gallium. Gallium oxides appeared on the free surface of gallium, whereas the gallium-HCl shows a shining and mirror-like surface. (b) Bulk-echo intensities measured in original gallium and HCl-treated gallium. The mean bulk echo intensities are spatially averaged over the region 20–100 mm from the transducer. After treating with HCl, the bulk-echo intensity became weaker.

[50]. Rayleigh scattering dominates when the object is much smaller than the ultrasound wavelength in the fluid. Mie scattering dominates when the object size is comparable to the ultrasound wavelength. Therefore, knowing the size of echoing objects can help us understand the mechanisms of ultrasound. As shown in Fig. 3 and S3, gallium oxide inclusions exist as single particles with diameters of a few microns, and also as agglomerations, with diameters of tens of microns. For 8 MHz ultrasound in gallium (wavelength 357 μm), if bulk echoes come mainly from single-particle inclusions, then we would expect Rayleigh scattering to dominate; if bulk echoes come mainly from agglomerations, then we would expect Mie scattering to dominate.

We calculated the diameters of echoing objects by measuring their terminal velocities and considering the forces on each echoing object, as described in the Methods. Velocities are indicated by the slopes of streaks like those shown in Fig. 5. When calculating diameters, we used the mean velocity measured from the small region between 4.5 and 5.5 cm from the transducer, where velocities are nearly uniform and forces other than those appearing in Eqs. (1) and (2) are presumably negligible. We first validated this estimation method in water. We measured object velocities acoustically with UDV and optically with PTV (Supplementary Fig. S1). The differences between UDV and PTV measurements were less than 7%. Inserting the UDV velocity measurements into Eqs. (1) and (2), we calculated the diameter to be 96–140 μm . The manufacturer specifies the diameter to be 100–130 μm , and the diameter we measured under an optical microscope is 108–122 μm . Both agree closely with the sizes calculated by measuring terminal velocities.

We cannot entirely rule out the presence of other forces. Thermal convection, in particular, can be driven in devices of this size by temperature differences well below 1 $^{\circ}\text{C}$. However, we did allow the water to equilibrate for a few hours before experiments. Moreover, the close agreement among size measurements from terminal velocity, optical size measurements, and supplier specifications suggest that terminal velocity can be used to estimate particle size with reasonable accuracy.

Having validated the method, we set out to measure the size of echoing objects in gallium. Using UDV velocity measurements in Eqs. (1) and (2), we calculated the mean diameter of gallium oxide inclusions as 58–64 μm . This size is larger than single gallium oxide particles, which suggests that echoing objects are typically agglomerations. However, this method assumes particles to be spherical and therefore only provides a rough estimate of the average size. Actual shapes and sizes surely vary. Thus, Mie scattering is likely the dominant mechanism producing ultrasound echoes in gallium, but Rayleigh scattering may also play an appreciable role.

3.3. Echo decay and signal deterioration

Next, we investigated echo decay and signal deterioration in UDV measurements, using the experimental apparatus shown in Fig. 2.

Fig. 7 presents a typical UDV echo map, where the echo intensities are measured over time and space. The strong peaks 110 mm from the transducer are caused by the specular reflection of ultrasonic waves at the back wall of the vessel, to be discussed below. The echoes measured in the bulk are from impurities suspended in the fluid. The figure shows that, in the bulk, echoes detected from greater distances are weaker. This phenomenon would result from both the attenuation of ultrasound when propagating in a pure liquid and the energy dissipation due to scattering by impurities. Fig. 7 also shows that bulk echo intensity decays with time. In gallium, this decay is likely due to a decrease over time in the

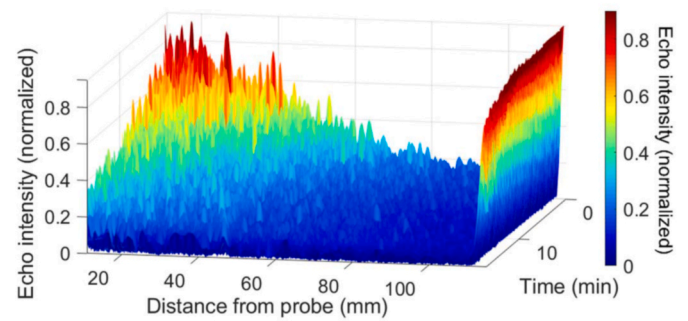


Fig. 7. A typical spatiotemporal UDV echo map. The strong peak at 110 mm represents the position of the back wall of container. Echo intensity decreases with distance and decays with time.

number of echoing objects in the ultrasound beam, since gallium oxide particles rise and heavier impurities sink. Below, these buoyancy effects will be considered further.

Since UDV velocity measurements are made from information contained in the echoes, echo intensity directly determines the quality of velocity measurements. Therefore, as bulk echoes decay with time, null and spurious velocity measurements become more likely. Fig. 8(a) clearly shows UDV measurement failure after a long measurement time. At 1 min, a smooth flow structure was measured; at 100 min, the same flow structure could still be recognized, but small fluctuations had appeared; at 150 min, the velocity profile had weakened substantially and was evidently much noisier; at 200 min, no meaningful velocity could be measured.

To evaluate the accuracy of UDV velocity measurements in a more straightforward way, we define the velocity deviation:

where $V_i(t)$ is the velocity profile at time t , $V_i(\text{mean})$ is the mean of the first 500 profiles (first 5 min), and the summation is taken over n measurement locations (here, all locations in the region 20 mm–100 mm from the transducer). The velocity deviation increases over time, as shown in Fig. 8(b), consistent with the fact that echo strength decreases over time, as shown in Fig. 7. Velocity deviation initially increases slowly (for the first 100 min), then increases rapidly, showing a nonlinear dependence on echo strength. When the velocity deviation is larger than about 0.5, our measurements capture no meaningful flow structure. Note that this is for a simple rotating flow; for a more complex flow, the UDV might fail to describe the flow structures at an even smaller velocity deviation value.

We performed several tests to study the mechanisms causing the deterioration and failure of UDV measurements in gallium. For each test, both the echo intensity and the velocity were measured. In Fig. 9, the top plots show the temporal evolution of mean bulk echo intensities from a series of continuous tests in gallium, where the mean bulk echo intensities are spatially averaged over the region 20–100 mm from the transducer. Initially, in test 1, we filled the vessel with gallium melt and performed UDV measurements with the transducer in direct contact with the melt. The bulk echo intensity decayed with time, as shown. The bottom plots in Fig. 9 show the corresponding velocity deviation calculated using Eq. (3), which increased as the echo intensity decayed. If the decay is caused by impurities sinking or rising out of the ultrasound beam path, bringing the impurities back should restore the bulk echo intensity, so in test 2, we manually stirred the gallium to mix

$$\text{Velocity deviation} = \frac{1}{n} \times \sum_{i=1}^n \sqrt{\left(\frac{V_i(t) - V_i(\text{mean})}{V_i(\text{mean})} \right)^2} \quad (3)$$

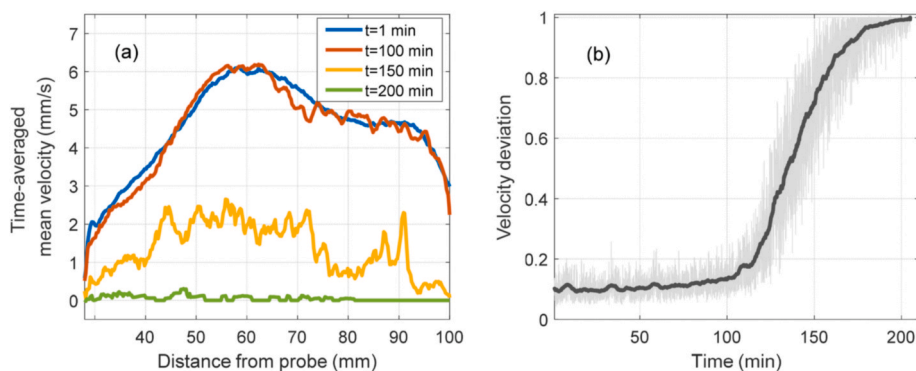


Fig. 8. UDV velocity measurement in gallium. (a) Velocity profiles measured at different times. Each velocity profile curve is the average of 1 min of measurements. (b) Velocity deviation vs. time. The flow was driven by a rotating magnetic field produced by a stir plate beneath the gallium container. As signals deteriorated over time, accurate velocity measurement became impossible.

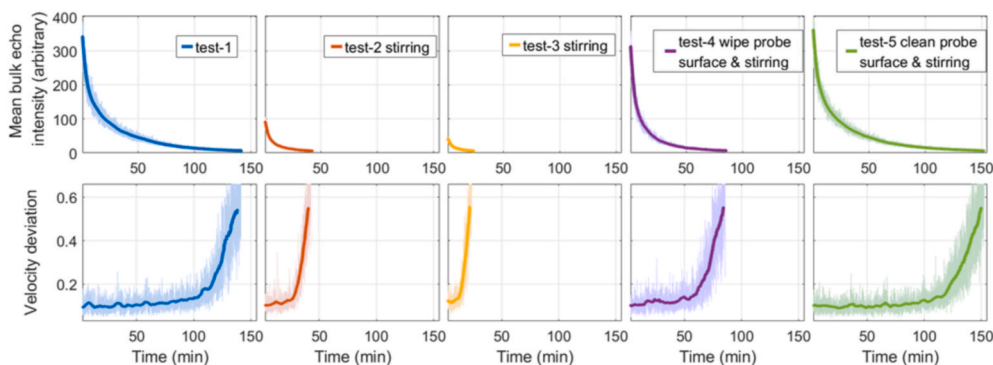


Fig. 9. Direct contact measurements: (top) mean intensity of bulk echo and (bottom) velocity deviation. For each test, the bulk echo intensity decays with time, and velocity deviation increases accordingly. Stirring (tests 2 and 3) improves echo intensity only weakly and extends the duration of viable velocity measurements only slightly. Wiping or cleaning the transducer surface (tests 4 and 5) improves echo intensity and extends velocity measurements much more.

impurities back into the bulk. However, as shown in the figure, the echo intensity grew only slightly, then quickly decayed, and velocity deviation quickly grew. We stirred the gallium again in test 3. As shown, the echo and velocity signals deteriorated even faster. These results suggest that the loss of echoing objects from the ultrasound beam path is not the only cause of UDV signal deterioration.

We then hypothesized that the deterioration of UDV signals is also caused by changes at the transducer surface. Continuing the same experiment, in test 4, we wiped the transducer surface with a cotton swab and manually stirred the gallium, then made more UDV measurements. Both the echo intensity and the velocity deviation improved substantially, as shown. In test 5, we poured the gallium out of the vessel, cleaned the ultrasound transducer surface, then filled the vessel with gallium again and restarted UDV measurement. As shown, the resulting echo intensity and velocity deviation almost matched test 1.

We hypothesize that the surface processes weakening UDV signals are related to the acoustic coupling and wetting between the ultrasound transducer and gallium. Ultrasound measurement requires a good acoustic coupling between the transducer and test liquid. Since metal melts usually have high surface tension, acoustic coupling with metal melts is determined not only by the acoustic impedance mismatch, but also by the wetting conditions between the transducer surface and the metal melt [7,8]. When pouring gallium out, we have observed a gallium oxide layer covering the transducer surface, perhaps caused by accumulation of gallium oxide particles that were circulating in the gallium. It is thermodynamically favorable for oxides to accumulate on the transducer surface, as the surface is a heterogeneous spot in the gallium melt (as is the vessel wall). As that oxide layer thickens over time, it may diminish wetting and acoustic coupling between the ultrasound

transducer and gallium [3,5,51]. If the wetting becomes very poor, small gaps (bubbles) might form and block the transmission of ultrasound waves. The vibration of the transducer surface when emitting ultrasound might also promote the formation of gaps. Any of these surface processes would substantially weaken UDV signals, regardless of the presence of echoing objects in the bulk. Signals might also be weakened if contaminants at the transducer surface form a layer thick enough to damp the ultrasound (on the order of a wavelength, or more), regardless of the acoustic coupling between the gallium and the contaminant layer. In that case, de-wetting would not be the relevant mechanism. However, we have not observed such thick layers.

Following the same procedure, we performed similar continuous tests in gallium with indirect-contact measurement, where the ultrasound signal was measured through a thin acrylic plate. The reason we selected acrylic is because it shows a better wettability to gallium, as shown in [Supplementary Fig. S5](#). In this case, the transducer did not contact gallium directly but was submerged in acoustic coupling gel. Consequently, the wetting and acoustic coupling conditions at the transducer surface were not subject to oxide accumulation and were therefore likely to be more stable over time. The results are shown in [Fig. 10](#). Unlike in the direct-contact case, stirring (test 2 and test 3) restored the echo intensity almost completely. Although gallium oxides visibly did attach to the acrylic plate surface, wiping the acrylic surface caused no obvious changes in the echo intensity or velocity deviation. The results from indirect-contact measurement suggest that when good wetting and acoustic coupling are maintained, stirring alone restores the bulk-echo intensity. Note that although the ultrasound signals deteriorate no further from test 2 to test 4, they are nonetheless weaker than in tests 1 and 5. To explain, we speculate that stirring did not mix bulk

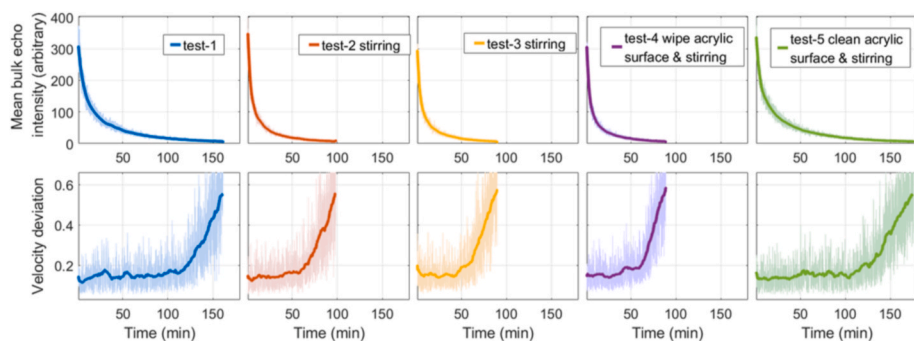


Fig. 10. Indirect contact measurement: (top) mean intensity of bulk echo and (bottom) velocity deviation. For each test, the bulk echo intensity decays with time, and velocity deviation increases accordingly. Stirring (tests 2 and 3) improves echo intensity and extends the duration of viable velocity measurements as much as wiping the surface (test 4), and much more than in the direct-contact case. Cleaning (test 5) improves echo intensity and extends velocity measurement more. After multiple tests, signal quality remained good.

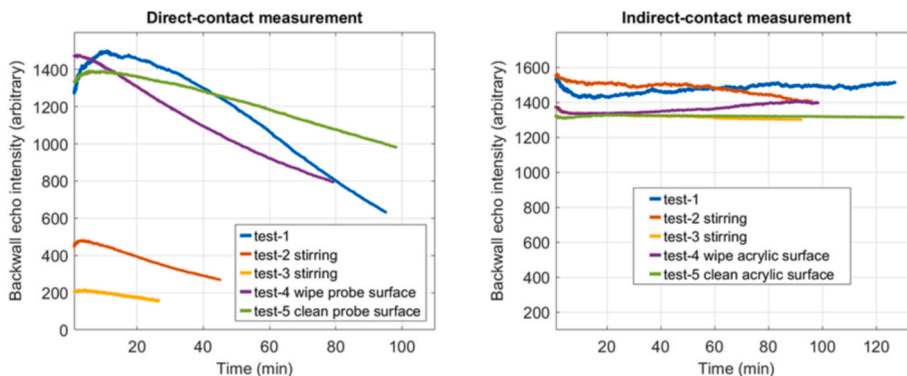


Fig. 11. Back-wall echo intensity for direct- and indirect-contact measurement. For direct-contact measurement, back-wall echo intensities decrease with time during each test. Wiping or cleaning the transducer surface (tests 4 and 5) restores the signal, but stirring (tests 2 and 3) has little effect. For indirect contact measurement, back-wall echo intensities remain strong regardless of stirring, wiping, cleaning, or the passage of time.

impurities as well as pouring and filling. The filling process could also induce microbubbles in the gallium melt, which would serve as additional echoing objects [7].

We can learn more about the role of acoustic coupling and wetting by measuring the intensity of echoes from the back wall of the vessel. Fig. 7 shows that the back-wall echo eventually decreases over time. It would be reasonable to expect the back-wall echo to increase, not decrease, over time, as particles leave the bulk fluid, thereby allowing more acoustic energy to reach the back wall. Observing the opposite, we are led to believe that some other mechanism has a stronger effect. We performed additional experiments to determine if wetting could explain. Fig. 11 shows the temporal evolution of back-wall echo intensity from a series of continuous tests in gallium. With direct-contact measurement, back-wall echo intensity decays over time during each test. As with the direct-contact measurements of bulk echo (Fig. 9), stirring does little to restore back-wall echo intensity (tests 2–3), but wiping or cleaning does much more (tests 4–5). With indirect-contact measurement, the back-wall echo intensity changes little over time and is hardly affected by stirring, wiping, or cleaning. Since bulk impurities apparently have little effect on back-wall echo, these measurements indicate that ultrasound signals can be significantly weakened by surface processes at the interface between the transducer and the metal melt.

From these results, we conclude that ultrasound signal deterioration results from two independent mechanisms: loss of echoing objects due to buoyancy, and wetting changes at the transducer surface. Stirring can mitigate the loss of echoing objects by mixing the melt and driving those objects back into the ultrasound beam path, as demonstrated in Fig. 10. Vigorous flows may provide enough mixing that manual stirring is entirely unnecessary. But even vigorous stirring is not sufficient for maintaining strong ultrasound signals through long experiments, as Figs. 8, 9 and 11 show; the effects of deteriorating wetting at the transducer interface must also be mitigated. Indirect-contact

measurement through a material that wets the metal melt well (e.g., acrylic with gallium, Supplementary Fig. S5) can help dramatically, as Figs. 10 and 11 show. Since accumulation of metal oxides seems to be one of the mechanisms that degrade wetting, techniques for slowing oxidation, such as maintaining an inert atmosphere (e.g., argon) [29,30,43,52], adding acid to the melt [5,20,43,44,52], or controlling oxidation electrochemically, might help keep signals strong and reliable. However, the role of oxide might be complicated: wetting may be best when there is neither too much nor too little oxide, as is the case for eutectic GaIn alloy [51]. Refining mitigation strategies is a fruitful topic for future research.

4. Conclusions

UDV is a powerful tool for measuring flow of opaque liquids, especially metal melts. Since UDV velocity measurements are made from information contained in bulk echoes, determining their sources and mechanisms is important for better use of ultrasound in metal melts.

In this study, we found different types of impurities in a gallium sample using SEM and EDS, including isolated gallium oxide particles a few microns in size, and agglomerations of oxide a few tens of microns in size. We used the UDV energy map to directly observe the movements of echoing objects in the fluid. Combining UDV energy maps and velocity profiles, we determined the oxide inclusions are the main source of bulk echoes in gallium. By measuring the terminal velocity of those inclusions, we estimated their mean size to be 58–64 μm , suggesting they are agglomerations, not single gallium oxide particles, and that ultrasound waves interact with them primarily via Mie scattering.

We performed series of UDV tests in gallium with either direct-contact measurement or indirect-contact measurement. Comparing the measured bulk echoes and back-wall echoes, we found that the deterioration of UDV measurements is caused by two independent

mechanisms: buoyancy causing echoing objects to rise or sink out of the ultrasound beam, and dwindling acoustic coupling at the transducer surface, probably due to oxide accumulation. Vigorous stirring can reduce or eliminate the first mechanism. Indirect-contact ultrasound measurement through a material that wets the melt well can reduce or eliminate the second mechanism. Using both techniques together can significantly extend the duration of high-quality UDV measurements.

Declaration of competing interest

The authors declare that they have no known competing financial interests or personal relationships that could have appeared to influence the work reported in this paper.

Acknowledgments

We thank URNano of the University of Rochester for the use of SEM and EDS facilities, R. Ibanez of the University of Rochester for help setting the PTV measurements, A. Allamore and A. Caldwell of Massachusetts Institute of Technology, and J.-C. Willemetz of Signal Processing for helpful conversations.

Appendix A. Supplementary data

Supplementary data to this article can be found online at <https://doi.org/10.1016/j.flowmeasinst.2021.102010>.

Funding

This work was supported by the National Science Foundation [award number CMMI-1562545].

References

- [1] Y. Takeda, Velocity profile measurement by ultrasound Doppler shift method, *Int. J. Heat Fluid Flow* 7 (4) (1986) 313–318.
- [2] Y. Takeda, Development of an ultrasound velocity profile monitor, *Nucl. Eng. Des.* 126 (2) (1991) 277–284.
- [3] S. Eckert, A. Cramer, G. Gerbeth, *Velocity Measurement Techniques for Liquid Metal Flows*, 2007.
- [4] Y. Takeda, Measurement of velocity profile of mercury flow by ultrasound Doppler shift method, *Nucl. Technol.* 79 (1) (1987) 120–124.
- [5] D. Brito, et al., Ultrasonic Doppler velocimetry in liquid gallium, *Exp. Fluid* 31 (6) (2001) 653–663.
- [6] S. Eckert, G. Gerbeth, Velocity measurements in liquid sodium by means of ultrasound Doppler velocimetry, *Exp. Fluid* 32 (5) (2002) 542–546.
- [7] A. Cramer, C. Zhang, S. Eckert, Local flow structures in liquid metals measured by ultrasonic Doppler velocimetry, *Flow Meas. Instrum.* 15 (3) (2004) 145–153.
- [8] R. Kazys, et al., High temperature ultrasonic transducers for imaging and measurements in a liquid Pb/Bi eutectic alloy, *IEEE Trans. Ultrason. Ferroelectrics Freq. Contr.* 52 (4) (2005) 525–537.
- [9] S. Eckert, G. Gerbeth, V.I. Melnikov, Velocity measurements at high temperatures by ultrasound Doppler velocimetry using an acoustic wave guide, *Exp. Fluid* 35 (5) (2003) 381–388.
- [10] Y. Ueki, et al., Velocity profile measurement of lead-lithium flows by high-temperature ultrasonic Doppler velocimetry, *Fusion Sci. Technol.* 60 (2) (2011) 506–510.
- [11] O. Andreev, Y. Kolesnikov, A. Thess, Application of the ultrasonic velocity profile method to the mapping of liquid metal flows under the influence of a non-uniform magnetic field, *Exp. Fluid* 46 (2009) 77–83.
- [12] J. Aubert, et al., A systematic experimental study of rapidly rotating spherical convection in water and liquid gallium, *Phys. Earth Planet. In.* 128 (1) (2001) 51–74.
- [13] L. Büttner, et al., Dual-plane ultrasound flow measurements in liquid metals, *Meas. Sci. Technol.* 24 (5) (2013), 055302.
- [14] S. Eckert, et al., Efficient melt stirring using pulse sequences of a rotating magnetic field: Part I. Flow field in a liquid metal column, *Metall. Mater. Trans. B* 39 (2) (2008) 374–386.
- [15] S. Franke, et al., Investigations of electrically driven liquid metal flows using an ultrasound Doppler flow mapping system, *Flow Meas. Instrum.* 48 (2016) 64–73.
- [16] T. Zürner, et al., Local Lorentz force and ultrasound Doppler velocimetry in a vertical convection liquid metal flow, *Exp. Fluid* 59 (1) (2017) 3.
- [17] M. Starace, et al., Ultrasound Doppler flow measurements in a liquid column under the influence of a strong axial current, *Magnetohydrodynamics* 51 (2015) 249–256.
- [18] R. Nauber, et al., Modular ultrasound velocimeter for adaptive flow mapping in liquid metals, in: *IEEE International Ultrasonics Symposium, IUS*, 2016.
- [19] G. Losev, R. Khalilov, I. Kolesnichenko, UDV study of a liquid metal vortex flow, *IOP Conf. Ser. Mater. Sci. Eng.* 208 (2017) 12022.
- [20] C. Zhang, et al., Intermittent behavior caused by surface oxidation in a liquid metal flow driven by a rotating magnetic field, *Metall. Mater. Trans. B* 42 (6) (2011) 1188–1200.
- [21] Y. Ueki, et al., Acoustic properties of Pb-17Li alloy for ultrasonic Doppler velocimetry, *Fusion Sci. Technol.* 56 (2) (2009) 846–850.
- [22] W. Yang, et al., Numerical study of flow motion and patterns driven by a rotating permanent helical magnetic field, *Metall. Mater. Trans. B* 47 (5) (2016) 2771–2784.
- [23] K. Timmel, S. Eckert, G. Gerbeth, Experimental investigation of the flow in a continuous-casting mold under the influence of a transverse, direct current magnetic field, *Metall. Mater. Trans. B* 42 (1) (2011) 68–80.
- [24] D. Schurmann, et al., Experimental study of the mold flow induced by a swirling flow nozzle and electromagnetic stirring for continuous casting of round blooms, *Metall. Mater. Trans. B* 50 (2) (2019) 716–731.
- [25] R. Nauber, et al., Novel ultrasound array measurement system for flow mapping of complex liquid metal flows, *Eur. Phys. J. Spec. Top.* 220 (1) (2013) 43–52.
- [26] R. Chaudhary, et al., Transient turbulent flow in a liquid-metal model of continuous casting, including comparison of six different methods, *Metall. Mater. Trans. B* 42 (5) (2011) 987–1007.
- [27] D. Schurmann, et al., Impact of the electromagnetic brake position on the flow structure in a slab continuous casting mold: an experimental parameter study, *Metall. Mater. Trans. B* 51 (1) (2020) 61–78.
- [28] P. Oborin, I. Kolesnichenko, Application of the ultrasonic Doppler velocimeter to study the flow and solidification processes in an electrically conducting fluid, *Magnetohydrodynamics* 49 (1–2) (2013) 231–236.
- [29] N. Thieme, et al., Ultrasound flow mapping for the investigation of crystal growth, *IEEE Trans. Ultrason. Ferroelectrics Freq. Contr.* 64 (4) (2017) 725–735.
- [30] K. Dadzis, et al., Directional melting and solidification of gallium in a traveling magnetic field as a model experiment for silicon processes, *J. Cryst. Growth* 445 (2016) 90–100.
- [31] I. Kolesnichenko, et al., Application of UDV for Studying the Flow and Crystallization of Liquid Metal in the Process of Electromagnetic Stirring, 2012.
- [32] J. Zeng, et al., A review of permanent magnet stirring during metal solidification, *Metall. Mater. Trans. B* 48 (6) (2017) 3083–3100.
- [33] A. Perez, D.H. Kelley, Ultrasound velocity measurement in a liquid metal electrode, *JoVE* 2015 (102) (2015) 1–12.
- [34] R.F. Ashour, et al., Competing forces in liquid metal electrodes and batteries, *J. Power Sources* 378 (2018) 301–310.
- [35] D.H. Kelley, D.R. Sadoway, Mixing in a liquid metal electrode, *Phys. Fluids* 26 (5) (2014) 57102.
- [36] B.E. Brawn, et al., Visualizing the invisible: ultrasound velocimetry in liquid sodium, *Chaos* 15 (4) (2005).
- [37] D.R. Sisan, et al., Experimental observation and characterization of the magnetorotational instability, *Phys. Rev. Lett.* 93 (11) (2004) 114502.1–114502.4.
- [38] D.S. Zimmerman, S.A. Triana, D.P. Lathrop, Bi-stability in turbulent, rotating spherical Couette flow, *Phys. Fluids* 23 (6) (1994).
- [39] T. Vogt, et al., Jump rope vortex in liquid metal convection, *Proceedings of the National Academy of Sciences - PNAS* 115 (50) (2018) 12674–12679.
- [40] D. Brito, et al., Zonal shear and super-rotation in a magnetized spherical Couette-flow experiment, *Physical review. E, Statistical, nonlinear, and soft matter physics* 83 (6) (2011).
- [41] N. Gillet, et al., Experimental and numerical studies of magnetoconvection in a rapidly rotating spherical shell, *J. Fluid Mech.* 580 (2007) 123–143.
- [42] N. Gillet, et al., Experimental and numerical studies of convection in a rapidly rotating spherical shell, *J. Fluid Mech.* 580 (2007) 83–121.
- [43] Y. Tasaka, Y. Takeda, T. Yanagisawa, Ultrasonic visualization of thermal convective motion in a liquid gallium layer, *Flow Meas. Instrum.* 19 (3) (2008) 131–137.
- [44] T. Vogt, et al., Detection of gas entrainment into liquid metals, *Nucl. Eng. Des.* 294 (2015) 16–23.
- [45] Z.H. Wang, et al., UDV measurements of single bubble rising in a liquid metal Galinstan with a transverse magnetic field, *Int. J. Multiphas. Flow* 94 (2017) 201–208.
- [46] K. Mader, et al., Phased array ultrasound system for planar flow mapping in liquid metals, *IEEE Trans. Ultrason. Ferroelectrics Freq. Contr.* 64 (9) (2017) 1327–1335.
- [47] S. Franke, et al., Ultrasound Doppler system for two-dimensional flow mapping in liquid metals, *Flow Meas. Instrum.* 21 (3) (2010) 402–409.
- [48] L.E. Kinsler, et al., *Fundamentals of Acoustics*, fourth ed., *Fundamentals of Acoustics*, 1999, p. 560.
- [49] J.C. Bailar, A.F. Trotman-Dickenson, *Comprehensive Inorganic Chemistry*, Oxford: Pergamon Press; distributed by Compendium Publishers, Elmsford, N.Y., 1973.
- [50] D.J. Lockwood, Rayleigh and Mie scattering, in: M.R. Luo (Ed.), *Encyclopedia of Color Science and Technology*, Springer New York, New York, NY, 2016, pp. 1097–1107.
- [51] M. Song, et al., Overcoming Rayleigh–Plateau instabilities: stabilizing and destabilizing liquid-metal streams via electrochemical oxidation, *Proc. Natl. Acad. Sci. Unit. States Am.* 117 (32) (2020) 19026.
- [52] T. Vogt, et al., Mixing enhancement in gas-stirred melts by rotating magnetic fields, *Metall. Mater. Trans. B* 43 (6) (2012) 1454–1464.

Bitong Wang is a PhD student of the Materials Science Program at the University of Rochester. Previously he earned a Master's degree of the Materials Science at the

University of Rochester and a Bachelor of Engineering degree of Metal Material Engineering at Sichuan University in China. His research areas include ultrasound, liquid metals, and liquid metal battery.

Douglas H. Kelley is an Associate Professor of Mechanical Engineering at the University of Rochester. He and his group study biophysical and technological fluid mixing, especially

cerebrospinal fluid flow in the brain and metal melt flows in liquid metal batteries and aluminum reduction cells. Doug earned a PhD from University of Maryland and did postdoctoral research at Yale University and MIT. He won a National Science Foundation CAREER Award, the University of Rochester's David T. Kearns Faculty Teaching and Mentoring Award, and the University's G. Graydon Curtis '58 and Jane W. Curtis Award for Nontenured Faculty Teaching.